Electronic Supporting Information (ESI) for "Synthesis, Electronic Transport and Optical Properties of Si:α-Fe_2O_3 Single Crystals"

Alexander J. E. Rettie,[a] William D. Chemelewski,[b] Bryan R. Wygant,[c] Jeffrey Lindemuth,[d] Jung-Fu Lin,[e,f] David Eisenberg,[g] Carolyn S. Brauer,[h] Timothy J. Johnson,[h] Toya N. Beiswenger,[h] Richard D. Ash,[i] Xiang Li,[b] Jianshi Zhou,[b] C. Buddie Mullins[a, b, c, *]

[a] McKetta Department of Chemical Engineering, The University of Texas at Austin, TX 78712 (USA)
[b] Texas Materials Institute, The University of Texas at Austin, TX 78712 (USA)
[c] Department of Chemistry, The University of Texas at Austin, TX 78712 (USA)
[d] Lake Shore Cryotronics, Westerville, OH 43082 (USA)
[e] Department of Geological Sciences, The University of Texas at Austin, TX 78712 (USA)
[f] Center for High Pressure Science and Technology Advanced Research (HPSTAR) Shanghai 201900 (China)
[g] Van 't Hoff Institute for Molecular Sciences, University of Amsterdam, Amsterdam, 1098 XH (The Netherlands)
[h] Pacific Northwest National Laboratory, Richland, WA, 99352 (USA)
[i] Department of Geology, University of Maryland, College Park, MD 20742 (USA)
[*] For correspondence: mullins@che.utexas.edu

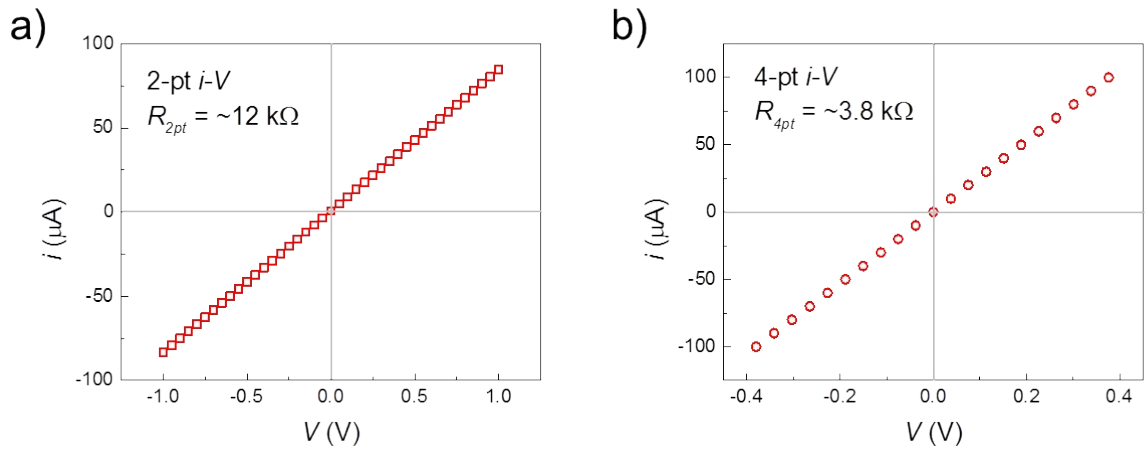

Figure S1: a) Example 2-pt and **b)** 4-pt *i-V* curves at room temperature. The contact material in this case was evaporated Ag.

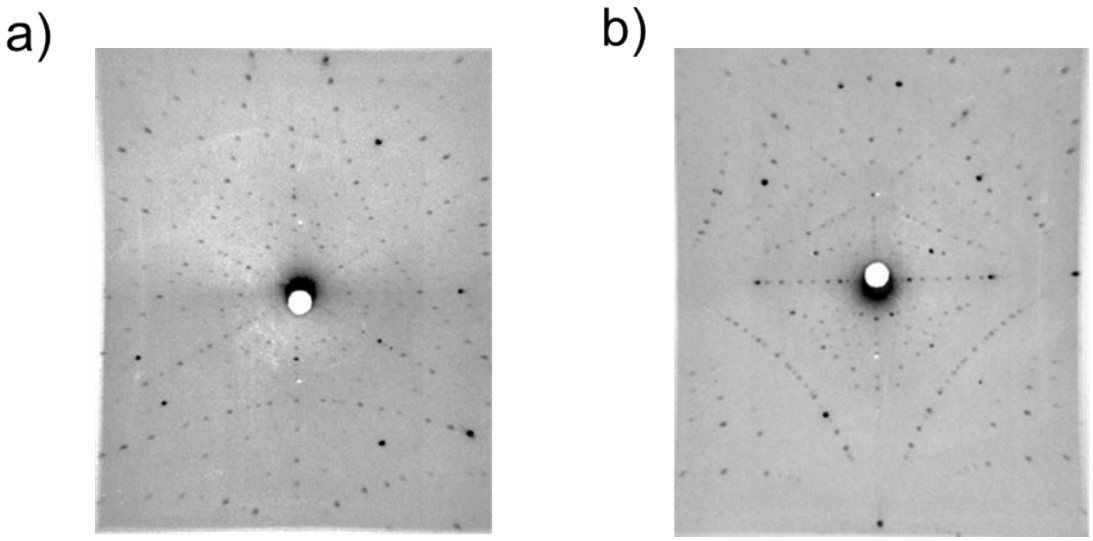

Figure S2: Representative patterns of Laue back-reflection XRD for **a)** (0001)-plane oriented and **b)** (1000)-plane Si:α-Fe_2O_3 single crystals.

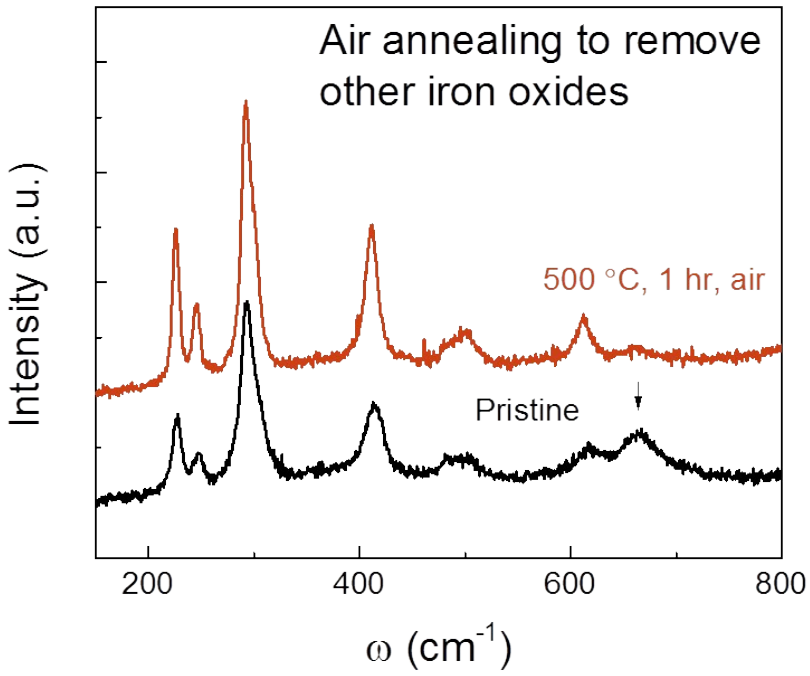

Figure S3: Raman spectra of one sample with small impurity peak (indicated by arrow at ~670 cm^{-1}) before and after thermal treatment (500 °C, 1 hr in air).

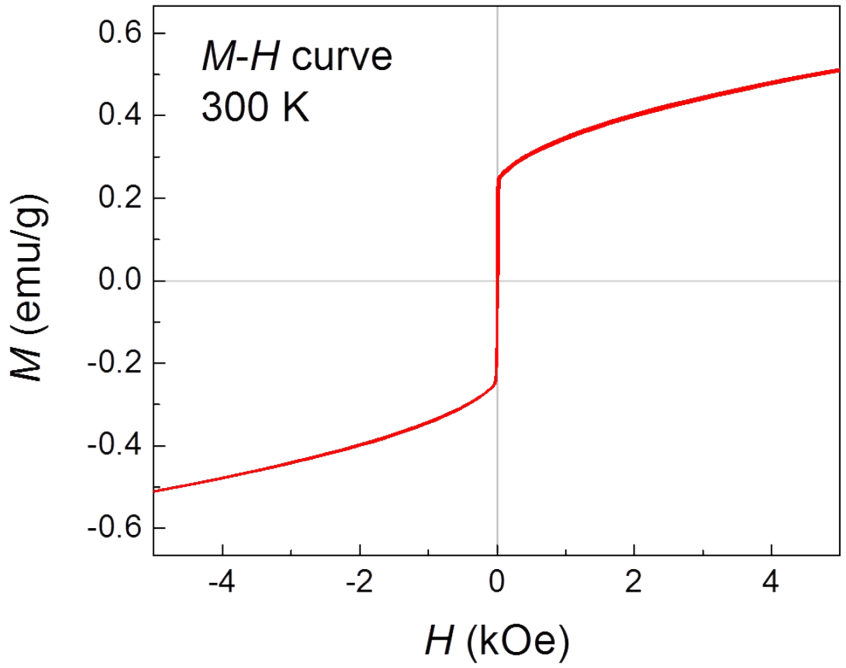

Figure S4: *M-H* curve for Si:α-Fe_2O_3 single crystal ([Si] = ~2×10^{19} cm^{-3}). The field was applied in the basal plane (easy axis), i.e. perpendicular to the *c*-axis.

S1 Crystal Composition

Crystal composition was determined by laser ablation inductively-coupled plasma mass spectrometry (LA-ICP-MS). Iron was used as internal standard, being 69.9% by mass of stoichiometric α-Fe_2O_3. Qualitative measurements that surveyed a wide range of transition and post-transition metal elements were used to narrow down the list of elements for quantification.

Of particular interest were elements that are common donor (e.g. Si^{4+}, Ti^{4+}, Ge^{4+}, Sn^{4+}, Nb^{5+}) or acceptor impurities (e.g. Cu^{2+}, Mg^{2+}) in hematite. These impurities likely come from trace impurities in the starting materials (α-Fe_2O_3, $TeCl_4$) and the samples represent different batches with different lots of chemicals used. Trace amounts of these elements were present, but the major impurity in all crystals was Si, the concentration of which ranged from 0.05-0.08% of the Fe sites and scaled with crystal conductivity (Table S1). Assuming the donor concentration, n to be equal to [Si] and using the resistivity equation for an n-type semiconductor: $\rho = 1/(ne\mu_d)$, an average drift mobility was calculated as ~5×10^{-3} cm^2 V^{-1} s^{-1} at room temperature. This is in good agreement with the estimated value of the drift mobility using the conductivity activation energy (~0.1 eV) of 10^{-2} cm^2 V^{-1} s^{-1}.

The calculated electron mobility was effectively constant over the range of doping measured. We utilized line scans over large (millimeter) areas of the samples during LA-ICP-MS to check uniformity and found that the Si concentration was highly homogenous across the crystals (the change being < 10%). This suggests that Si was incorporated via the vapor phase during growth (as we postulated in the main text), and not via diffusion from the SiO_2 walls, which would have resulted in a strong concentration gradient in the crystals.

Table S1: Sample composition and room temperature resistivity.

Sample	ρ at 300 K (Ω-cm)	[Si] / [Fe] (at.%)	[Si] ≈ N_d (cm^{-3})	μ_d ($cm^2 V^{-1} s^{-1}$)	Minor impurities (ppm)
1	58.7	0.05	1.9×10^{19}	5.5×10^{-3}	Ti (2), Ge (2), Sn (2.5), Cu (28)
2	52.3	0.07	2.7×10^{19}	4.4×10^{-3}	Ti (3.4), Ge (5.5)
3	49.6	0.06	2.3×10^{19}	5.4×10^{-3}	Ti (18.5), Ge (13.2), Cu (2.7)
4	35.5	0.08	3.3×10^{19}	5.4×10^{-3}	Ti (5), Ge (2), Mo (5)

S2 Calculation of adiabatic pre-factor, $\sigma_0 T$

Equation S1 was used to calculate $\sigma_0 T$ using the parameters listed in Table S2:

$$\sigma_0 T = N_d e^2 g a^2 v_0 / k_B \qquad \text{(S1)}$$

where, T is the absolute temperature, N_d is the concentration of donor impurities, e is the electronic charge, a is the hopping distance, v_0 is characteristic phonon frequency and k_B is the Boltzmann constant. The geometric pre-factor, g was determined using vector analysis.[1] The Fe atom geometry is six-fold rings in the basal plane with each ion having 3 nearest neighbors, approximately 3 Å away. g was calculated as 0.75. A v_0 value of 1.85×10^{13} Hz was used, corresponding to the highest energy longitudinal phonon mode in hematite[2] (mode at ~620 cm^{-1} in the Raman spectrum, Figure S3).

Table S2: Pre-factor calculation parameters for samples 1 and 4 in Table S1.

Sample	g (-)	N_d (cm^{-3})	a (Å)	v_0 (Hz)	$\sigma_0 T$ (S cm^{-1} K)		
					Calculated	Data (WFS)	Data (AFS)
1	0.75	1.9×10^{19}	3.0	1.85×10^{13}	440	199 ± 1	2721 ± 26
4	0.75	3.3×10^{19}	3.0	1.85×10^{13}	764	463 ± 2	5279 ± 34

S3 Infrared Absorption Fitting

The difference in the infrared reflectance (ΔR) between the undoped α-Fe_2O_3 powder was determined using fityk software (version 0.9.8). The broad infrared absorption in both cases was

similar and could be acceptably fit using 2 Gaussian peaks centered at ~0.4 and ~0.8 eV, shown in Figure S5. The y-axis has been transformed as (100 - ΔR) so the difference is positive. From conductivity and Seebeck measurements we know that $(E_a - t) = \sim 100$ meV. Using the adiabaticity criterion we can solve to obtain a lower limit for t,[3]

$$t^2 >> (E_a k_B T/\pi)^{1/2} (h\nu_0/\pi) \qquad \text{(S2)}$$

where, h is Planck's constant. At room temperature, $t >> \sim 30$ meV, thus setting a lower limit for the peak of a small-polaron absorption feature of ~0.5 eV.

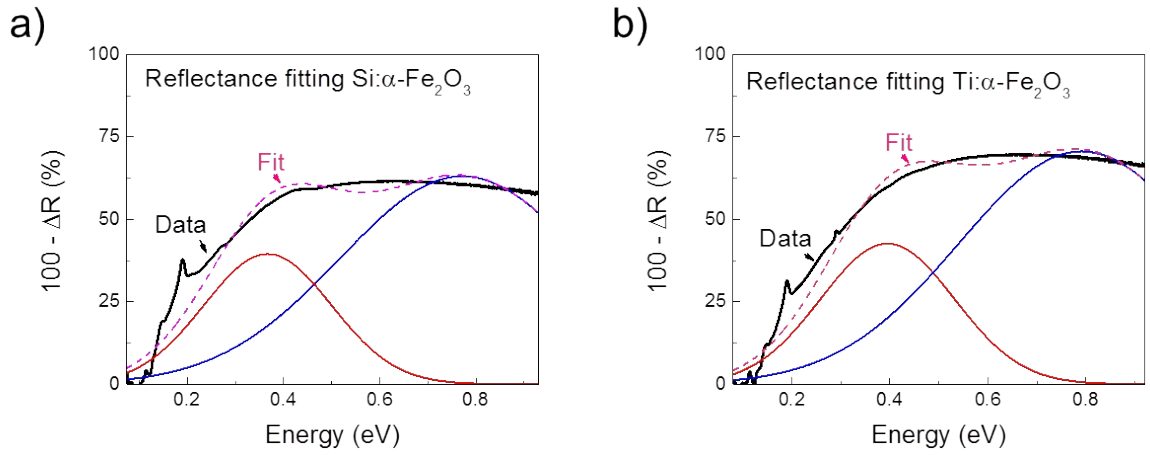

Figure S5: Differential reflectance spectra between undoped α-Fe_2O_3 and **a)** pulverized Si-α-Fe_2O_3 crystals and **b)** 2% Ti-α-Fe_2O_3 powder synthesized by a solid state method. The raw data is presented in the main text in Figure 11a. The data, fit components and overall fit are represented by solid black, red, blue and dashed magenta lines respectively.

References

1. A. J. E. Rettie, W. D. Chemelewski, J. Lindemuth, J. S. McCloy, L. G. Marshall, J. Zhou, D. Emin and C. B. Mullins, *Appl. Phys. Lett.*, 2015, **106**, 022106.
2. N. Iordanova, M. Dupuis and K. M. Rosso, *J. Chem. Phys.*, 2005, **122**, 144305-144305-144310.
3. D. Emin and T. Holstein, *Ann. Phys.*, 1969, **53**, 439-520.